European Journal of Pharmaceutics and Biopharmaceutics 227 (2026) 115182

Contents lists available at ScienceDirect

European Journal of Pharmaceutics and Biopharmaceutics

journal homepage: www.elsevier.com/locate/ejpb

Research paper

A smarter dermal filler: Antimicrobial protection and collagen stimulation with niacinamide

Alexandre Porcello [a], Cindy Schelker [a], Olivier Jordan [b,c], Karl Perron [b,c,d], Emmanuelle Sublet [b,c], Cintia Cristina Santi Martignago [b,c,e], Cíntia Marques [a], Lee Ann Applegate [f,g,h], Alexis Emmanuel Laurent [i,**], Viorica Patrulea [b,c,*]

[a] Development Department, LOUNA REGENERATIVE SA, CH-1228 Plan-les-Ouates, Switzerland
[b] Institute of Pharmaceutical Sciences of Western Switzerland, University of Geneva, 1 Rue Michel Servet, CH-1211 Geneva, Switzerland
[c] School of Pharmaceutical Sciences, University of Geneva, 1 Rue Michel Servet, CH-1211 Geneva, Switzerland
[d] Department of Plant Sciences, Microbiology Unit, University of Geneva, CH-1205 Geneva, Switzerland
[e] Department of Biosciences, Federal University of São Paulo (UNIFESP), Silva Jardim Street, 136, Santos, SP 11015020, Brazil
[f] Faculty of Biology and Medicine, University of Lausanne, CH-1015 Lausanne, Switzerland
[g] Center for Applied Biotechnology and Molecular Medicine, University of Zurich, CH-8057 Zurich, Switzerland
[h] Oxford OSCAR Suzhou Center, Oxford University, 215123 Suzhou, China
[i] Manufacturing Department, LAM Biotechnologies SA, CH-1066 Epalinges, Switzerland

ARTICLE INFO

Keywords:
Anti-inflammatory
Antibacterial
Biostimulation
Collagen
Dermal filler
Hyaluronic acid
Niacinamide
Skin aging

ABSTRACT

Biological skin aging involves structural changes, including flattening of the epidermal-dermal junction and reduced collagen types I and III. Modern aesthetic medicine is shifting from volumetric enhancement toward regenerative dermal fillers, though risks of delayed inflammation or infection from post-procedural injections should be mitigated. Niacinamide is a well-established molecule that stimulates collagen synthesis, modulates inflammation and inhibits bacterial growth.

We evaluated the biostimulatory, antimicrobial, anti-inflammatory, and safety profiles of a new niacinamide-enriched cross-linked hyaluronic acid dermal filler (HAR) compared to untreated controls and Belotero Balance® (commercial reference). Biostimulation was assessed *ex vivo* in human skin explants cultured for 8 days, using Masson's trichrome staining and collagen I/III immunostaining. Antibacterial activity against Gram-positive and Gram-negative bacterial models was assessed by monitoring growth, while anti-inflammatory properties were analyzed *via* TNF-α and IL-6 levels in LPS-stimulated macrophages. Safety and biocompatibility were evaluated against human dermal fibroblasts.

HAR-treated explants displayed improved epidermal architecture and a denser collagen type I network. HAR inhibited bacterial growth (~90% Gram-negative; ~50% Gram-positive), significantly lowered IL-6 and TNF-α levels, and showed excellent biocompatibility with high fibroblast viability and minimal hemolysis. These findings highlight HAR as a multifunctional dermal filler combining essential structural support with regenerative, antibacterial, and anti-inflammatory benefits.

1. Introduction

The aesthetic medicine field has recently shifted from simple volumetric enhancement toward treatments that provide long-lasting effects and dermal tissue rejuvenation. Unlike traditional hyaluronic acid (HA)-based fillers, modern dermal fillers are increasingly expected to demonstrate intrinsic skin regeneration, including the stimulation of *de novo* collagen and elastin synthesis [1]. The structural integrity of the extracellular matrix (ECM) is essential to maintain healthy skin. Fibrillar collagens, primarily types I, III, and V, represent the main structural proteins of the dermal matrix, and dermal fibroblasts are the principal cells responsible for the production of this fibrillar collagen [2]. Among these, collagen type I constitutes approximately 80% of the dermal ECM across various ages and plays a central role in maintaining skin firmness,

* Corresponding author.
** Corresponding author.
E-mail addresses: alexis.laurent@lambiotechnologies.com (A.E. Laurent), viorica.patrulea@unige.ch (V. Patrulea).

https://doi.org/10.1016/j.ejpb.2026.115182
Received 20 April 2026; Received in revised form 20 June 2026; Accepted 11 July 2026
Available online 12 July 2026

resilience, and mechanical strength [2–5]. Collagen type III, although less abundant in adult skin, represents roughly 8–11% of the dermal matrix and contributes to skin elasticity and tissue repair [6]. Together, collagens I and III, and elastin are essential for preserving skin structural integrity and a youthful appearance of the skin [3].

Biological skin aging is characterized by progressive structural and functional modifications within the dermis that ultimately manifest as visible surface changes [4]. These age-related processes contribute to noticeable differences in skin texture, elasticity, and overall integrity between younger and older individuals [7]. Aging compromises the structural integrity of fibrillar collagen through a combination of intrinsic cellular senescence and extrinsic exposure to solar ultraviolet (UV) radiation, including both dermal-penetrating UVA and epidermal-penetrating UVB rays [6,8]. These factors collectively induce severe oxidative stress and inflammation, overwhelming the skin's natural defense mechanisms and leading to excessive production of reactive oxygen species (ROS) and inflammatory mediators [9].

Oxidative stress and inflammation further disrupt key cellular signaling pathways, particularly the mitogen-activated protein kinase (MAPK) and nuclear factor κB (NF-κB) cascades [9]. As a result, the expression of ECM-related genes and the structural integrity of key ECM proteins are altered, leading to loose, wrinkled, and aged skin due to reduced collagen synthesis and accelerated degradation. Of note, dermal fibroblasts play a central role in this process, as they represent the primary source of matrix metalloproteinases (MMPs) involved in collagen breakdown during intrinsic aging [9,10]. Morphologically, youthful skin is typically characterized by a thicker epidermis and a highly dense, compact dermal architecture featuring well-defined gaps between collagen fibers. In stark contrast, aged skin displays a thinner epidermis and a less dense dermis with fragmented and disorganized collagen fibers [11,12]. A hallmark of skin aging is the flattening of the epidermal-dermal junction due to the loss of the interdigitating undulations known as rete ridges. This structural flattening is accompanied by a severe reduction in collagen content, particularly collagen type I, leading to decreased dermal density and increased fragmentation of the ECM [13]. Although biostimulatory treatments targeting collagen I may not always dramatically increase overall collagen quantities, they can significantly improve the organization and quality of the dermal matrix.

Despite the regenerative potential of modern dermal fillers, aesthetic procedures inherently involve creating percutaneous micro-injuries. This mechanical disruption of the epidermal barrier may temporarily alter the native skin microbiota and trigger mild inflammatory responses, potentially leading to early, late, and delayed post-procedure complications [14]. Among the microbial species of concern, *Staphylococcus aureus* represents a common skin Gram-positive bacterium, while Gram-negative non-skin contaminants may also be introduced during needle-based administration procedures [14–16]. Furthermore, tissue trauma, ROS, and UV radiation can stimulate inflammatory responses in resident fibroblasts and keratinocytes [17]. In the dermal microenvironment, macrophages play a key role in this inflammatory process by synthesizing and releasing pro-inflammatory cytokines, primarily tumor necrosis factor-alpha (TNF-α) and interleukin-6 (IL-6) [18–20]. If not properly controlled, this inflammatory cascade can exacerbate tissue degradation and contribute to premature skin aging [20]. Therefore, strategies aimed at reducing macrophage-derived cytokine production may help to alleviate localized inflammation following clinical aesthetic procedures.

To address these complex requirements, niacinamide (water-soluble vitamin B3) has gained prominence as a versatile, multifunctional molecule in anti-aging cosmetic skincare. Niacinamide possesses well-documented biostimulatory capabilities, specifically the ability to induce the synthesis of collagen types I, III, and V [19,21,22]. Additionally, it exhibits significant anti-inflammatory properties, largely through modulation of the poly(ADP-ribose) polymerase-1 (PARP-1) enzyme. The targeted inhibition of PARP-1 downregulates nuclear factor kappa B (NF-κB) transcription, leading to a marked decrease in the levels of secreted pro-inflammatory cytokines, including TNF-α and IL-6 [23,24]. Niacinamide also offers notable localized antibacterial activity against several pathogens. This bactericidal effect may occur through direct mechanisms by interfering with bacterial DNA and causing cell cycle arrest, thus blocking bacterial proliferation [23,25], or indirectly *in vivo* by activating the skin's innate immune system through increased production of antimicrobial peptides (AMPs) [26].

Given the distinct properties of HA and vitamin B3, there is a strong rationale for evaluating composite formulations. By adding niacinamide into a cross-linked HA matrix, two major limitations of conventional fillers can be addressed: the lack of intrinsic antimicrobial activity and the limited stimulation of endogenous collagen synthesis. As such, this approach has the potential to meet an important unmet clinical need in aesthetic medicine by providing fillers that not only restore volume but also enhance tissue regeneration while reducing the risk of bacterial complications. In this study, we investigated HAR, a novel dermal filler designed for subcutaneous administration, consisting of a cross-linked HA matrix blended with niacinamide. By embedding niacinamide within the hydrogel network, this formulation aims to provide immediate physical effects while allowing for gradual *in situ* release of the molecule as the matrix naturally degrades, thus supporting long-term antioxidant and anti-aging benefits. This work builds upon our previous studies in which we evaluated various HAR prototypes and assessed their capacity to stimulate collagen production in human dermal fibroblasts (HDFs) *in vitro*. Those investigations demonstrated that specific HA–niacinamide ratios and network architectures can modulate fibroblast activity and enhance collagen synthesis, providing the mechanistic basis for the present formulation strategy [22].

The primary objective of this study was to evaluate the biostimulatory potential of HAR through an *ex vivo* investigation using human skin explants, focusing on its impact on epidermal architecture, dermal remodeling, and collagen matrix reorganization. For the first time, this study provides a characterization of the integrated biological responses to a niacinamide-enriched, cross-linked HA filler within a physiologically relevant human skin model, thereby providing a more translational assessment of its regenerative capacity. In addition, a comparative analysis was performed against a widely used and standard HA filler, Belotero Balance®, as well as standard formulations containing different concentrations of niacinamide. This approach further enabled a systematic evaluation of HAR's antimicrobial activity against *Escherichia coli* and *Staphylococcus aureus*, its anti-inflammatory capacity through suppression of TNF-α and IL-6 secretion in a stimulated murine macrophage model, and the specific impact of niacinamide concentration on HDF activity.

2. Materials and Methods

2.1. Materials

Test Articles and Comparators. The investigational product, HAR (Shape and Volume), a commercial dermal filler, was obtained from LOUNA AESTHETICS (Poisy, France) and was used as the primary test formulation. Each 1 mL syringe contains 15 mg of HA, 7.5 mg of vitamin B3 (niacinamide), and 3 mg of lidocaine. HAR is a proprietary dermal filler comprising a cross-linked HA matrix blended with niacinamide.

Belotero Balance® (Merz Aesthetics/Anteis SA, Plan-les-Ouates, Switzerland), a standard, commercially available dermal filler was used as the primary reference comparator. In addition, free (unencapsulated) niacinamide (Cooper, Melun, France) was tested as a control compound across multiple assays to distinguish the effects of the active compound from those of the hydrogel formulation.

For antibacterial assays, a standard broad-spectrum antibiotic, like gentamicin sulfate (PanReac AppliChem, Darmstadt, Germany), was used as a positive control to represent maximal growth inhibition.

Biological Models and Cell Lines. Human full-thickness skin explants (reference: P3105-AB40), with an average diameter of 11 mm (±

1 mm), were harvested from surgical abdominoplasty residues obtained from a 40-year-old female donor (Fitzpatrick skin color scale phototype II). Primary HDFs (DECH-SK), originally isolated from a 12-week-old male donor, were ethically sourced from the Regenerative Therapy Unit at the Centre Hospitalier Universitaire Vaudois (CHUV, Lausanne, Switzerland).

The murine macrophage cell line RAW 264.7 (ATCC® TIB-71™) was obtained from the American Type Culture Collection (ATCC, Manassas, VA, USA). Bacterial strains utilized for the antimicrobial assays included the Gram-negative *Escherichia coli* (ATCC 25922) and the Gram-positive *Staphylococcus aureus* (ATCC 29213, ATCC, MN, Virginia, USA). Defibrinated sheep blood, utilized for the hemocompatibility assays, was acquired from BioConcept Ltd. (Allschwil, Switzerland).

Culture Media and Reagents. Tissue explants were maintained in BIO-EC's Explants Medium (BEM). Bacterial strains were cultured and hydrated using Mueller-Hinton Broth (MHB). Mammalian cell lines/types were cultured in adapted Dulbecco's Modified Eagle Medium (DMEM). DMEM was appropriately supplemented with fetal bovine serum (FBS), 1% penicillin/streptomycin, and 1% L-glutamine, all of which were sourced from Gibco (Thermo Fisher Scientific, Waltham, Massachusetts, USA).

Cell washing and dilution protocols utilized standard phosphate-buffered saline (PBS) and 1× Dulbecco's phosphate-buffered saline (DPBS). To induce the pro-inflammatory M1 macrophage phenotype, lipopolysaccharide (LPS) derived from *E. coli* serotype O26:B6 was procured from Sigma-Aldrich (St. Louis, Missouri, USA). A 1% sodium dodecyl sulfate (SDS) solution served as the cytotoxic positive control for cell viability assays. Absolute ethanol (Merck, Zug, Switzerland) was utilized for chromophore stabilization in the hemolysis assay.

Antibodies and Assay Kits. For immunofluorescence labeling, the primary polyclonal anti-collagen I antibody (ref. ab138492-1001) was procured from Abcam (Cambridge, UK), while the Alexa Fluor 488-conjugated secondary antibody (ref. A11008) was obtained from Life Technologies (Carlsbad, California, USA). Cellular nuclei were counterstained using propidium iodide. Immunohistochemical detection of type III collagen utilized a primary polyclonal anti-collagen III antibody (ref. 1330-01) from SBD (Birmingham, Alabama, USA). A standard biotin/streptavidin amplification system was employed in conjunction with the VIP peroxidase substrate kit (ref. SK-4600) from Vector Laboratories (Newark, California, USA). Pro-inflammatory cytokines were quantified utilizing murine-specific enzyme-linked immunosorbent assay (ELISA) kits for TNF-α (DY410) and IL-6 (DY406), both manufactured by Biotechne (R&D Systems, Zug, Switzerland).

2.2. Physicochemical Characterization

2.2.1. Scanning Electron Microscopy (SEM) and Critical Point Drying

To preserve the porous network structure and minimize collapse during drying, we used a critical point drying (CPD) procedure. Briefly, we dehydrated the hydrogel in acetone for 10 minutes, then immersed it in pure ethanol for another 20 minutes. The samples were then carefully placed in the specimen chamber of the CPD (Tousimis Research Corporation, Rockville, Maryland, USA). Following this, ethanol was replaced with liquid CO_2 through several exchange cycles according to the manufacturer's protocol. The samples were brought above the critical point of CO_2 (31.1 °C and 73.8 bar), and then slowly depressurized to obtain the dried hydrogels while preserving their porous network.

Then, CPD-dried samples were stored in a desiccator until SEM preparation. For SEM, samples were mounted on aluminum stubs and sputter-coated with a 5 nm gold layer using a Leica EM SCD500 sputter coater. Images were acquired using a JEOL JSM-7001F (JEOL Ltd., Tokyo, Japan) operated at an accelerating voltage of 5 kV.

2.2.2. Rheological Characterization and Cohesivity Assessment

The storage modulus (G′) and the loss modulus (G″) of HAR and Belotero Balance® were experimentally determined in oscillatory rheology using an HR 10 rheometer (TA Instruments, Guyancourt, France) equipped with a 40-mm-diameter Peltier plate–plate measuring system. The G′ and G″ values were obtained within the linear viscoelastic region (LVR) of the amplitude sweep. The amplitude sweep was set at 3 N/m^2. All measurements were performed at 1 Hz and 22 °C on volumes of 0.6 mL of each product. A sample hood was used during the measurements in order to minimize sample evaporation. The experimental G′ and G″ values were determined using three experimental replicates in all the assays. Tan δ values were calculated as the ratio of G″ to G′. In addition, G′ values were measured after 12 and 24 months of real-time stability storage (25 ± 2 °C, 60 ± 5% relative humidity, protected from sunlight).

Cohesivity was assessed using the drop-weight method as an indirect measure. Syringes equipped with a 30 G needle were used and the hydrogels were extruded at a constant speed of 12 mm/min. After a stable extrusion force was reached, at least six drops were collected and weighed to determine the mean drop weight. Measurements were performed in triplicate.

2.3. Biostimulation Assays

To evaluate the biostimulatory effects of the HAR dermal filler, an *ex vivo* human skin model was utilized. Nine full-thickness skin explants, each with an average diameter of 11 mm (± 1 mm), were harvested from abdominal surgical residues. The use of human surgical waste tissue for this study strictly adhered to the ethical principles outlined in the Declaration of Helsinki and was conducted in full compliance with Article L.1243-4 of the French Public Health Code. In accordance with these specific regulations, the utilization of discarded surgical residues does not mandate prior approval from an institutional ethics committee.

Following preparation, the nine explants were randomly assigned to three distinct experimental groups: three explants served as baseline tissue controls (Day 0), three were designated as untreated controls which were maintained over the study period, and three received intradermal injections of the HAR hydrogel. For the treated group, 50 μL of HAR was injected directly into the dermal matrix using standardized syringes and 30 G needles, while approximating the injection depth of 2–3 mm. The explants were subsequently maintained in survival *ex vivo* culture within multi-well plates, submerged in 2 mL of BEM medium to ensure optimal tissue viability. Incubation was carried out in a controlled environment at 37 °C within a humidified atmosphere containing 5% CO_2. Throughout the 8-day experimental timeline, the untreated control explants received no intervention other than routine culture medium replenishment. Specifically, 1 mL of the BEM culture medium, representing half of the total well volume, was systematically renewed on Day 1, Day 4, and Day 6.

On Day 0, the three baseline control explants were harvested and bisected to establish initial tissue parameters. One half of each explant was immediately fixed in buffered formalin for conventional histology, while the remaining half was flash-frozen and stored at –80 °C for subsequent immunolabeling. An identical harvesting and bisection protocol was applied to the remaining untreated and HAR-treated explants upon the conclusion of the 8-day incubation period. For general histological assessment, the formalin-fixed samples underwent a 24-hour fixation period before being subjected to automated dehydration and paraffin wax impregnation utilizing a Leica PEARL tissue processor. The processed tissue biopsies were then precisely embedded in paraffin blocks using a Leica EG 1160 embedding station. Serial 5-μm-thick sections were cut with a Leica RM 2125 Minot-type microtome and permanently mounted onto Superfrost® histological glass slides. To evaluate the general morphology of the epidermal and dermal architectures, the formalin-fixed paraffin-embedded (FFPE) sections were stained using the Goldner variant of Masson's trichrome. Additionally, basal cellular viability across the explants was routinely monitored *via* direct microscopical observation.

To quantify specific ECM alterations, targeted immunostaining was

performed on the frozen tissue fractions. The cryopreserved samples were sectioned into 7-µm-thick slices utilizing a Leica CM 3050 cryostat and securely mounted onto salinized Superfrost® Plus glass slides to ensure optimal tissue adhesion during the staining procedures. Immunofluorescence labeling for type I collagen was executed using a primary polyclonal anti-collagen I antibody (Abcam, ref. ab138492-1001). The primary antibody was diluted to 1:1600 in a blocking PBS buffer supplemented with 0.3% bovine serum albumin (BSA) and 0.05% Tween® 20 and was incubated for 1 h at ambient temperature. The targeted signal was subsequently fluorometrically revealed using an Alexa Fluor 488-conjugated secondary antibody (Life Technologies, ref. A11008), while the cellular nuclei were counterstained with propidium iodide to provide vital histological context. For the immunohistochemical detection of type III collagen, sections were similarly incubated for 1 h at ambient temperature with a primary polyclonal antibody (SBD, ref. 1330-01), diluted at 1:200 in PBS containing 0.3% BSA. This signal was enhanced using a robust biotin/streptavidin amplification system and visually resolved using Vector VIP (Vector, ref. SK-4600), a peroxidase substrate that precipitates to form a distinct violet stain upon oxidation. All subsequent histological and immunostaining evaluations were documented through rigorous microscopical observation, utilizing a Leica DMLB, an Olympus BX43, or an Olympus BX63 microscope. High-resolution digital photomicrographs were consistently captured using a numeric DP Olympus camera integrated with cellSens image analysis and storing software (Olympus). For both collagen I and collagen III immunostaining, a semi-quantitative analysis was performed with the ImageJ software (National Institutes of Health, Bethesda, Maryland, USA) on nine images. Briefly, the color channels were split and the green channel was retained. The fluorescence mean for each photograph was obtained through the Isodata algorithm [27]. Collagen I and III expression was scored based on histological slides with a scale ranging from 1 to 7 (1 – very weak; 2 – weak; 3 – moderate; 4 – fairly clear; 5 – clear; 6 – very clear; 7 – strong). Scoring was performed in a blinded manner by one independent pathologist.

2.4. Antibacterial Activity Assessments

To evaluate the antibacterial efficacy of HAR in comparison with the reference dermal filler Belotero Balance®, we followed the bacterial growth by measuring optical density at 600 nm after 24 h of incubation with HAR, Belotero Balance®, or free niacinamide at various concentrations [28]. The assays were performed against two clinically relevant bacterial strains frequently implicated in post-procedural dermal complications: the Gram-negative *E. coli* and the Gram-positive *S. aureus*.

To better mimic physiological tissue hydration and product behavior *in vivo*, hydrogel samples were first subjected to a lyophilization step directly in the assay microplates prior to bacterial exposure. Briefly, 100 µL aliquots of each hydrogel formulation were dispensed into the wells of a standard 96-well plate. Following complete lyophilization (Telstar LyoBeta, Terrasa, Spain), the dehydrated hydrogel matrices were reconstituted and uniformly hydrated by the addition of 100 µL of MHB culture medium.

Concurrently, standardized bacterial inoculums were prepared by adjusting the microbial suspensions to a 0.5 McFarland standard turbidity, ensuring a consistent starting bacterial density. These standardized suspensions were subsequently diluted 1:100 in fresh MHB, and 100 µL of the resulting bacterial suspension was systematically inoculated into each test well containing the hydrated hydrogels.

Robust experimental controls were established to validate the assay's dynamic range. A gentamicin-free bacterial culture served as the positive growth control (0% inhibition), while sterile MHB medium without bacterial inoculation functioned as the negative assay control to ensure an absence of baseline contamination. The fully assembled 96-well plates were then statically incubated for 24 hours at a physiological temperature of 37 °C. To benchmark the antimicrobial activity against an established clinical standard, gentamicin was utilized as a reference control for *E. coli* and *S. aureus*, respectively.

Following the 24-hour incubation period, the antibacterial activity was quantified turbidimetrically [29]. The percentage of bacterial growth inhibition was calculated by normalizing the OD_{600} values of the treated samples against the predefined assay controls. Specifically, the values were normalized between the untreated positive growth control (0% inhibition) and the gentamicin-treated control at a defined concentration of 1 µg/mL for *E. coli* and 4 µg/mL for *S. aureus* (100% inhibition). The normalization of the percentage of inhibition was mathematically derived using the following equation:

$$\% \text{ Inhibition} = \frac{OD_{GC} - OD_{Sample}}{OD_{GC} - OD_{Genta}} \times 100$$

Where OD_{GC} represents the absorbance of the untreated bacterial growth control, OD_{Sample} represents the absorbance of the hydrogel-treated test sample, and OD_{Genta} denotes the absorbance of the maximal antibiotic inhibition control.

2.5. Anti-inflammatory Activity Assessments

To quantitatively evaluate the anti-inflammatory properties of the hydrogel formulations, an *in vitro* enzyme-linked immunosorbent assay (ELISA) was performed using a standardized murine macrophage model. RAW 264.7 murine macrophages were continuously cultured in T-75 tissue culture flasks (Corning, USA). The growth medium consisted of Dulbecco's Modified Eagle Medium (DMEM) supplemented with 10% fetal bovine serum (FBS), 1% penicillin/streptomycin, and 1% *L*-glutamine. To maintain optimal phenotypic stability, the culture medium was rigorously refreshed every three days. Subculturing was systematically performed upon the cells reaching approximately 80% confluency. To ensure biological consistency and reproducible functional responses, all subsequent experimental procedures exclusively utilized cells precisely at passage level 5. For the assay setup, the macrophages were harvested and seeded into 96-well tissue culture plates at a defined density of 1×10^4 cells per well, utilizing a 100 µL cell suspension volume.

Prior to cellular treatment, conditioned medium extracts from the hydrogel samples were systematically prepared in strict accordance with ISO 10993-12 guidelines for the biological evaluation of medical devices. The extraction vehicle consisted of complete DMEM supplemented with a reduced serum concentration of 5% FBS. Briefly, 400 µL aliquots of each respective hydrogel sample were transferred into microtubes containing 4 mL of the extraction medium. These mixtures were uniformly homogenized by vortexing for 20 seconds and subsequently incubated at 72 °C under continuous agitation for a 24-hour period to ensure comprehensive molecular elution. Following this accelerated incubation, the resulting hydrogel extracts were aseptically purified by filtration through 0.22 µm pore-size membranes and immediately utilized for cellular interventions to prevent the degradation of labile compounds.

To mimic a localized inflammatory response, the adhered macrophages were stimulated with 1 µg/mL of LPS, which was diluted in DMEM containing 5% FBS. The cells were exposed to this endotoxin for 12 hours to robustly induce cellular polarization toward the pro-inflammatory M1 macrophage phenotype. Following this activation phase, the LPS-laden medium was completely aspirated and replaced with 200 µL of the freshly prepared, sterile-filtered hydrogel conditioned medium. All experimental conditions were rigorously performed in independent triplicates to ensure statistical reliability. The experimental setup included a negative baseline control consisting of non-polarized, unstimulated cells, alongside a positive inflammatory control comprising LPS-polarized macrophages maintained strictly in standard medium (DMEM with 5% FBS) without any exposure to the hydrogel extracts.

The immunomodulatory impact of the hydrogel extracts was determined by quantifying the secretion of key pro-inflammatory cytokines in

the culture supernatants. Commercially available sandwich ELISA kits specific to murine TNF-α (DY410) and IL-6 (DY406) (Biotechne, R&D Systems, Zug, Switzerland) were utilized strictly according to the manufacturer's operational instructions. High-affinity polystyrene microplates were initially coated overnight at ambient temperature with highly specific target-capture monoclonal antibodies. Following a rigorous blocking step with PBS to prevent non-specific binding and a subsequent washing cycle, the collected cellular supernatants were introduced into the functionalized wells and incubated for 2 hours at ambient temperature. The microplates were then thoroughly washed again and incubated for an additional hour with biotinylated secondary detection antibodies. The colorimetric reaction was quantified by measuring the sample optical density at a wavelength of 450 nm using a precision BioTek Microplate Reader (BioTek, Luzern, Switzerland). Final cytokine concentrations were accurately interpolated from highly characterized standard curves and expressed as picograms of cytokine per milliliter of supernatant (pg/mL).

2.6. Biocompatibility and Safety Assessments

To comprehensively evaluate the *in vitro* safety profile and cellular biocompatibility of the formulated hydrogels, targeted cytotoxicity assessments were conducted using primary human dermal fibroblasts (DECH-SK cell type). For the quantitative WST-1 and qualitative Live/Dead viability assays, the human dermal fibroblasts (HDFs) were precisely seeded into transparent or optically clear black-walled 96-well microplates (Corning®, Corning, New York, USA). The initial seeding densities were optimized at 5×10^4 cells/mL for the colorimetric assays and 5×10^3 cells/mL for fluorescence imaging. The cellular monolayers were cultured under standard physiological conditions and allowed to grow for 24 hours to ensure complete adherence and confluence prior to experimental intervention. Following this critical stabilization period, the standard culture medium was completely aspirated and gently replaced with 100 μL of the respective hydrogel solutions, which had been previously diluted at a 1:10 ratio in DMEM.

Cellular viability and morphological integrity were systematically evaluated at defined chronological endpoints, specifically on Days 3 and 5 post-exposure. To ensure robust assay validity, a highly cytotoxic 1% sodium dodecyl sulfate (SDS) solution (Bio-Rad, Hercules, California, USA) was utilized as a definitive negative control for cell survival. Quantitative cell viability was determined utilizing the WST-1 colorimetric assay (Roche, Basel, Switzerland). The metabolic capacity of viable cells was quantified by measuring the differential absorbance at 450 nm against a reference wavelength of 690 nm using a precision BioTek Microplate Reader (BioTek, Luzern, Switzerland). These absorbance values were subsequently normalized against untreated control populations, maintained in DMEM supplemented with 10% FBS, at the Day 3 endpoint to calculate relative viability percentages.

Qualitative morphological viability was evaluated using a dual-fluorescence Live/Dead staining kit (Merck, Darmstadt, Germany) incorporating 2 μM calcein AM and 4 μM ethidium homodimer-1. The cells were incubated with this dual-staining solution at 37 °C for 15 minutes, in accordance with the manufacturer's instructions. High-resolution fluorescence imaging of the stained cell populations was subsequently captured using an advanced ImageXpress Micro-4 automated imaging system (Molecular Devices, San Jose, California, USA), utilizing an Andor Zyla 4.2 camera and processed *via* the MetaXpress software (v.6.6.1.42). To ensure statistical robustness and reproducibility, all viability and cytotoxicity experiments were independently performed in triplicate.

To further ascertain the hemocompatibility of the hydrogel formulations, a rigorous *in vitro* hemolysis assay was conducted to evaluate potential lytic activity against mammalian erythrocytes [28]. Freshly obtained, defibrinated sheep blood (BioConcept Ltd., Allschwil, Switzerland) was gently washed three times in 1× Dulbecco's Phosphate-Buffered Saline (DPBS) to isolate the red blood cells (RBCs) and remove free plasma components, followed by dilution to a standardized final working concentration of 5%. Concurrently, the selected hydrogel samples were diluted in PBS at a 1:1 volumetric ratio and aliquoted into a flat-bottom 96-well microplate. For the active assay phase, 50 μL of the purified 5% sheep RBC suspension was added to 50 μL of the diluted hydrogel preparations within a separate round-bottom 96-well plate to promote optimal cell-material contact. These sample mixtures were subsequently incubated for 30 minutes at ambient temperature under continuous, gentle agitation utilizing an Orbit LS shaker (model S2030-LS-B) to prevent localized erythrocyte sedimentation. Following incubation, the assay plates were centrifuged at 4000 rpm for 10 minutes to safely pellet the intact erythrocytes. The resulting supernatants, containing any released hemoglobin from lysed cells, were carefully aspirated. Subsequently, 50 μL of each harvested supernatant was transferred to a fresh flat-bottom 96-well plate and thoroughly mixed with 250 μL of absolute ethanol *per* well to stabilize the chromophore. The precise extent of hemoglobin release was ultimately quantified spectrophotometrically by measuring the absorbance values at the specific wavelengths of 412 nm and 700 nm.

2.7. Statistical Analysis

All quantitative experimental data are expressed as the mean ± standard deviation (SD), derived from a minimum of three independent biological replicates ($n = 3$) to ensure robust analytical reproducibility. Statistical evaluations to ascertain significant differences among multiple experimental groups were comprehensively executed using a one-way analysis of variance (ANOVA). To stringently control Type I error rates across multiple group comparisons, specific post-hoc analyses were systematically applied in accordance with the experimental design. For the antimicrobial growth inhibition assessments, the primary one-way ANOVA was subsequently followed by Tukey's multiple comparisons post-test to evaluate differences between all group means. Conversely, for the quantification of anti-inflammatory cytokine markers (TNF-α and IL-6) via ELISA, Bonferroni's multiple comparisons post-test was strictly utilized. Statistical significance was established *a priori* at an alpha level of 0.05. Within the graphical representations and corresponding text, specific significance thresholds are denoted as follows: * $p \leq 0.05$, ** $p \leq 0.005$, *** $p \leq 0.001$, and **** $p \leq 0.0001$ relative to their respective predefined control groups.

3. Results

3.1. Physicochemical Design Considerations of HAR

The current market of HA-based dermal fillers comprises a wide range of injectable products. Regulatory guidelines typically require manufacturers to disclose the total concentrations of HA and lidocaine in their products. However, other important parameters, such as the degree of chemical modification and key rheological properties, like the storage modulus, are not systematically required to be reported. Despite this variability in disclosure, most commercially available crosslinked HA fillers from major manufacturers are based on 1,4-butanediol diglycidyl ether (BDDE) as the crosslinking agent. This approach is used in well-known brands such as Teosyal RHA®, Restylane®, Belotero®, and Juvéderm® [30].

CPD drying following sequential precipitation in acetone and ethanol yielded HAR hydrogels with a highly regular network of fibrous, needle-like structures (Fig. 1A). This morphology was notably different from that typically observed in conventional freeze-dried HA samples. Since our goal was to preserve the hydrogel structure as closely as possible to its native hydrated state, we evaluated several drying approaches. Sequential precipitation in acetone followed by absolute ethanol was found to be the most effective method, maintaining the overall microstructure while minimizing structural collapse. In contrast, samples precipitated directly in ethanol (data not shown) exhibited substantial

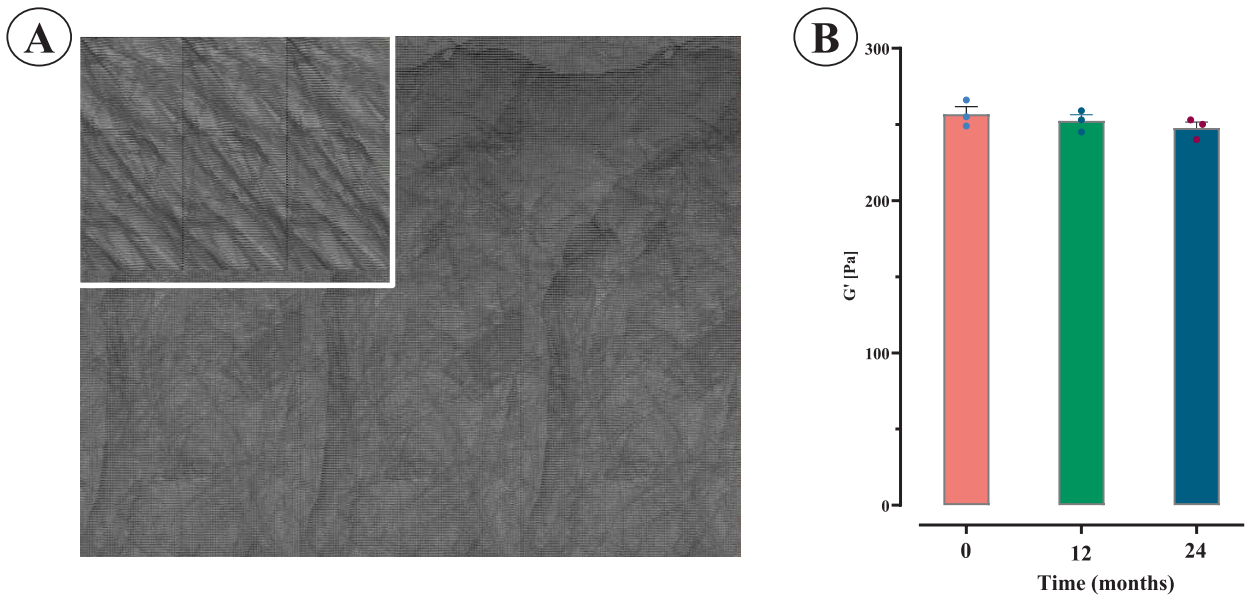

Fig. 1. Physicochemical characterization of the HAR hydrogel. A) Morphological images of the HAR hydrogel in dried state following the CPD process (scale bar = 50 μm and for the insert, 5 μm), and B) Long-term stability of the HAR hydrogel over 24 months, assessed by monitoring the storage modulus (G′).

collapse of the network and a marked loss of the characteristic HAR architecture.

As for the rheological behaviour, reported degrees of modification for these products typically range from approximately 2 to 10%, while storage modulus values may vary broadly, between 20 and 1100 Pa, depending on the product and its intended clinical indication [31,32]. Most of the HA fillers on the market are composed solely of the cross-linked HA matrix and do not contain additives. A few exceptions exist, for example, Stylage® from Laboratoire Vivacy incorporates mannitol as an antioxidant, and the manufacturer Neauvia uses poly(ethylene glycol) (PEG)-based epoxy crosslinkers and includes amino acids such as glycine and proline [30,33].

In the present study, we investigated a new formulation referred to as HAR, defined as "HA Reticulated", consisting of a BDDE-crosslinked HA hydrogel supplemented with vitamin B3 (niacinamide). From a formulation perspective, HAR was technically benchmarked against the Belotero® reference and analyzed to evaluate its physicochemical and biological properties. The HA raw material used for HAR production displayed an intrinsic viscosity of 2.5 m^3/kg, determined according to the European Pharmacopoeia (chapter 2.2.9), indicating a high-molecular-weight starting polymer. From a clinical standpoint, HAR was designed primarily for injection into the superficial fat compartments (SFC) or the deep dermis. Belotero Balance® was included in this study exclusively as a commercial comparator for *in vitro* evaluation and was not evaluated in the *ex vivo* analyses or considered for clinical comparison (Table 1).

HAR (*i.e.*, Shape and Volume), part of the Louna Fillers product range, is indicated for the restoration and sustained preservation of soft, natural volume in the SFCs. The formulation contains 17.5 mg/mL HA, supplemented with 7.5 mg/mL niacinamide and 3.0 mg/mL lidocaine. The HA is BDDE-crosslinked with a reported degree of chemical modification of 3.9%, and the gel is manufactured using the proprietary Boost and Fusion technology [22]. Rheological characterization at 1 Hz showed a storage modulus (G′) of 256 ± 8 Pa, indicating a structured and predominantly elastic gel network (tan δ ≈ 0.12) capable of providing superficial mechanical support while remaining adaptable to surrounding tissues.

For comparison, Belotero Balance® (Merz Aesthetics, Switzerland), from the Belotero® product range, contains 22.5 mg/mL BDDE-crosslinked HA with a higher reported degree of modification (5.7%) and does not include niacinamide or lidocaine [32]. The product is manufactured using the Cohesive Polydensified Matrix® (CPM) technology and is clinically indicated for the correction of nasolabial folds, tear trough deformities, marionette lines, perioral lines, oral commissures, and chin wrinkles. Despite its higher HA concentration and greater crosslinking degree, Belotero Balance® exhibits a substantially lower storage modulus (G′ = 50 ± 4 Pa at 1 Hz), indicating a softer and

Table 1
Technical overview and rheological properties of the HA-based dermal filler products included in the experimental study.

Product Commercial Name	HAR - Shape and Volume	Belotero Balance®
Company name	Louna Aesthetics	Merz Aesthetics
Product range	Louna Fillers	Belotero®
Intended Product Uses[1]	Restoration and preservation of soft tissue, volume in the SFC or the deep dermis of the face	Injection into the mid-to-deep dermis for the correction of moderate-to-severe facial wrinkles and folds
HA Concentration (mg/mL)	17.50	22.50
Niacinamide Concentration (mg/mL)	7.50	0
Lidocaine Concentration (mg/mL)	3.00	0
Cross Linker	BDDE	BDDE
Degree of HA Modification (%)	3.67	5.7[2]
Manufacturing Technology	Boost and Fusion	CPM*
Needle Gauge (G)	30 or 27	30
Storage modulus (G′) in Pa at 1 Hz and 22 °C	256 ± 8	50 ± 4
Loss modulus (G″) in Pa at 1 Hz and 22 °C	31 ± 2	33 ± 2
Loss tangent (tan δ = G″/G′) at 1 Hz and 22 °C	≈ 0.12	≈ 0.66

* Cohesive Polydensified Matrix (CPM), [1]Belotero Balance instructions for use, [2][32]

more flowable gel optimized for superficial wrinkle correction and smooth tissue integration.

From a rheological standpoint, HAR demonstrates an approximately five-fold higher storage modulus than Belotero Balance®, suggesting increased elastic resistance and a stronger capacity for structural support within superficial adipose compartments. While higher polymer crosslinking is generally associated with increased gel stiffness and prolonged *in vivo* persistence, this comparison underscores that rheological behaviour cannot be predicted from the HA concentration or the crosslinking degree alone [31,32]. Instead, the internal gel architecture, mediated by factors such as crosslinker distribution, network homogeneity, and manufacturing technology, plays a critical role in determining its macroscopic viscoelastic behavior.

Of note, niacinamide is not expected to participate in covalent crosslinking within the BDDE-modified HA network. Rather, as a small hydrophilic molecule, it may interact with HA through reversible non-covalent interactions, particularly hydrogen bonding with the available carboxyl (-COOH) and hydroxyl (-OH) groups of HA. Through its nitrogen atom from the pyridine ring and the 3-carboxamide (-$CONH_2$) group, niacinamide may promote intermolecular associations within the hydrated matrix, potentially influencing water re-organization and polymer chain mobility [22,34]. These non-covalent interactions can modulate the viscoelastic behavior of the gel and contribute to an increase in key rheological parameters, including the storage modulus, without altering the underlying covalent crosslink density [22].

Beyond the reported moduli, cohesivity provides complementary insights into how the gel deposit behaves once injected and subjected to natural mechanical constraints in the skin tissue. Assessed by the drop-weight method (*i.e.,* 30 G needle, 12 mm/min), HAR yielded a mean drop weight of 40.6 ± 0.8 mg (n = 3), reflecting consistent internal cohesion across replicates. This relatively high cohesivity is in line with the non-covalent, hydrogen-bonding contribution of niacinamide [22]. As the measured extrusion force depends strongly on extrinsic factors, such as syringe ergonomics, needle gauge and geometry, and plunger/injection speed, a reliable and clinically meaningful assessment therefore requires a dedicated standardized methodology, which we addressed previously in a separate study [22,30].

Importantly, the storage modulus remained stable under real-time storage conditions, with G′ values of 248 ± 7 Pa after 24 months versus 256 ± 8 Pa at baseline, confirming the long-term viscoelastic stability of the formulation (Fig. 1B). Such stability assessment is a mandatory requirement for any commercial injectable hydrogel product, ensuring that its functional properties are maintained throughout its shelf life.

It is also important to note that regulatory labelling guidelines require manufacturers to disclose the total HA concentration of a given product, but this parameter does not distinguish between crosslinked and non-crosslinked (linear) HA fractions. Many commercial fillers consist of biphasic or multiphasic systems in which crosslinked HA is combined with varying amounts of linear HA to modulate injectability, rheological properties, cohesivity, and tissue integration. For this reason, the total HA concentration alone is not a sufficient predictor of the rheological properties or clinical performance of a defined dermal filler.

3.2. Collagen I/III and Dermal Remodeling Induced by HAR

The biostimulatory capacity of the HAR hydrogel was evaluated following preliminary *in vitro* investigations demonstrating increased total collagen synthesis in primary dermal fibroblasts exposed to the formulation [22]. This enhanced collagen production was largely attributed to the strategic integration of vitamin B3 (niacinamide), which is known to stimulate ECM protein expression [35].

To assess whether these findings translate to a more physiologically relevant context, HAR was evaluated *ex vivo* using full-thickness human skin explants harvested from a healthy 40-year-old female donor. The structural impact of the dermal filler on skin architecture was initially visualized through rigorous, blinded histological examination of tissue biopsies stained with Masson's trichrome (Goldner variant, Fig. 2A).

At baseline (Day 0), untreated control explants exhibited a characteristically mature architecture, featuring pronounced epidermal undulations and a distinctly irregular stratum corneum (Fig. 2A). Furthermore, the dermo-epidermal junction displayed well-defined rete ridges, indicating a highly irregular, physiological epidermal topography. After 8 days of *ex vivo* culture without treatment, epidermal undulations appeared moderately reduced, although the rete ridges remained clearly visible, suggesting only limited structural changes under the culture conditions. Nevertheless, the rete ridges remained distinctly identifiable, suggesting that the intrinsic culture conditions provided only a limited, spontaneous smoothing effect.

In contrast, skin explants treated with HAR for 8 days presented the most regular thickness (Fig. 2B) and structurally refined epidermal architecture among all tested conditions. The outer epidermal contour appeared smoother and more linear, with a profound reduction in surface micro-relief. Accompanying this surface smoothing, the dermo-epidermal junction exhibited greater uniformity, characterized by an increase in the density of the papillary dermis, with a highly organized collagen network. Collectively, these morphological observations suggest that HAR treatment imparts an effect on the epidermal surface while actively fortifying the structural organization of the underlying dermis compared to both untreated baseline (Blank at Day 0) and chronological controls (Blank at Day 8).

To examine the induced ECM remodeling at the molecular level, targeted immunofluorescence staining specific for type I collagen was subsequently performed on the cryopreserved tissue sections. Negative control sections processed without the primary collagen I antibody showed no fluorescent signal, unequivocally confirming the specificity of the assay (Fig. 3A). In the baseline (Day 0), the epidermal layer appeared structurally uneven. The underlying collagenous boundary was highly irregular, resulting in an indistinct and structurally abrupt transition at the epidermal-dermal junction.

Within the deep dermis of these baseline samples, the type I collagen matrix appeared dense but displayed a highly heterogeneous spatial distribution, characterized by discrete areas of extreme focal accumulation interspersed with sparse, disorganized, and thickened fibrillar structures. In the untreated Day 8 control explants, the dermo-epidermal surface achieved a slightly smoother but persistently wavy topography, while collagen type I fibers organized into denser aggregates, yet maintained an irregular spatial distribution throughout the matrix.

In contrast, explants treated with HAR for 8 days exhibited a thicker and more homogeneous epidermis. The dermal layer contained a densely packed, uniformly distributed type I collagen network consisting of thinner, highly organized fibers, reflecting highly structured and rejuvenated ECM. Additionally, to confirm these profound morphological improvements, semi-quantitative analysis indicated a higher signal for type I collagen in HAR-treated tissues compared to the Day 0 (blank) baseline, although this increase did not reach statistical significance (Fig. 3B). A blinded and independent expert scoring confirmed these findings: collagen levels were moderate at Day 0, slightly declined in the untreated Day 8 explants, and were notably enhanced after HAR treatment (Fig. 3C). Surprisingly, a drop in collagen content was observed in untreated explants after 8 days, whereas HAR-treated explants showed a significant increase in type I collagen production over the same period.

Following the assessment of type I collagen, the dynamic expression and spatial distribution of type III collagen, a key marker of tissue repair and skin elasticity, were investigated *via* targeted immunohistochemistry. Negative control sections confirmed assay specificity, showing no detectable collagen III signal (Fig. 4A). At baseline (Day 0), the type III collagen network appeared loose, fragmented and irregularly distributed, with large interstitial gaps, collectively evidencing an ECM of critically diminished density accompanied by an irregular dermo-epidermal boundary.

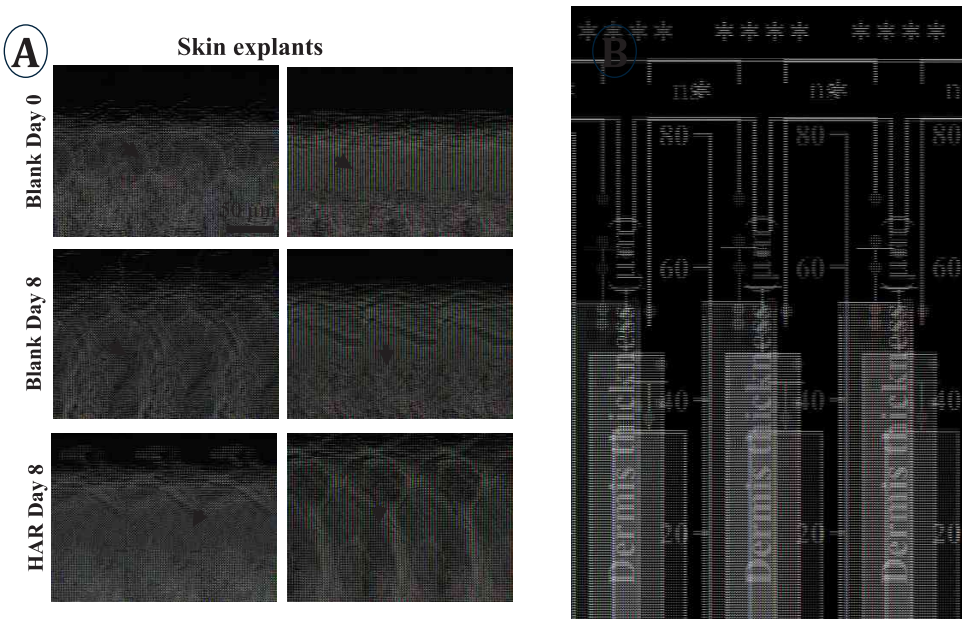

Fig. 2. Dermal thickness assessment in skin explants. A) Photomicrograph of skin explants stained with Masson's trichrome (Goldner variant) at Day 0 with blanks, after 8 days of culture without treatment, and after 8 days with HAR treatment. Black arrows indicate collagen distribution in the papillary dermis. Scale bar = 50 μm. B) Dermal thickness measurement at Day 0 with blanks, after 8 days of culture without treatment, and after 8 days with HAR treatment (n = 9; *ns* = not significant, * $p \leq 0.05$, and **** $p \leq 0.0001$).

After 8 days of *ex vivo* culture, untreated control tissues developed a comparatively denser and more organized type III collagen matrix, with fewer gaps and more uniform fibrillar distribution at the epidermal-dermal junction. In contrast, HAR-treated explants over the same 8-day period yielded a highly dense, uniform, and tightly packed type III collagen matrix. The corresponding epidermal-dermal junction in the HAR-treated samples appeared remarkably smooth and structurally continuous.

Similar to the quantitative findings for type I collagen, the semi-quantitative densitometric assessment of the type III collagen staining revealed no statistically significant difference in absolute fluorescence intensity between the HAR-treated samples and the control explants (Fig. 4B). Expert evaluation of tissue explants indicated that collagen production, initially assessed as ranging from moderate to fairly clear at Day 0 and Day 8 (Fig. 4C), demonstrated a marked increase by Day 8 in the HAR-treated explants. This resulted in collagen III production being classified between fairly clear and clear.

3.3. Antibacterial Activity

To evaluate the protective properties of HAR in potential post-procedural infection, we tested the direct antibacterial activity against two clinically relevant pathogens: *E. coli*, a Gram-negative bacterium (Fig. 5A), and *S. aureus*, a Gram-positive opportunistic skin pathogen (Fig. 5B).

Bacterial growth was measured after 24 h of exposure to different concentrations of free niacinamide, the HAR hydrogel, which comprises cross-linked HA functionalized with niacinamide, and Belotero Balance®, a standard HA dermal filler. The aminoglycoside antibiotic gentamicin, administered at respective defined concentrations of 1 μg/mL and 4 μg/mL, was used as a positive control for functional comparison.

The quantitative analysis revealed that free niacinamide showed intrinsic concentration-dependent antibacterial activity. At the highest tested concentration (15 mg/mL), free niacinamide strongly inhibited *E. coli*, matching gentamicin's effect, but showed minimal impact on *S. aureus*. When the concentration of free niacinamide was reduced by half to 7.5 mg/mL, its inhibitory capacity diminished to 35% for *E. coli* and a negligible 10% inhibition for *S. aureus*.

Though free niacinamide showed limited efficacy at 7.5 mg/mL, which is the same concentration found in HAR, the fully formulated HAR hydrogel demonstrated potent and selective antibacterial effects. After 24 h of exposure, ~90% inhibition of *E. coli*, comparable to gentamicin, but only moderate growth inhibition (~50%) of *S. aureus* was obtained. Belotero Balance® (commercial control) was significantly less effective, reducing *E. coli* growth by only 30%, while its effect on *S. aureus* was similar to HAR (~50% growth inhibition). These results highlight HAR's *in situ* protection potential against Gram-negative bacteria, with moderate activity against Gram-positive strains. Since the hydrogel is designed as an injectable dermal filler, its antimicrobial activity is expected to provide localized protection at the implantation site, thereby helping to reduce the risk of bacterial colonization and infection within the dermal layer.

3.4. Safety and Biocompatibility

To evaluate the safety profile and *in vitro* biocompatibility of the investigated dermal fillers, cytotoxicity assays were performed using human dermal fibroblasts (HDFs). Initial morphological evaluations were carried out using a fluorescence Live/Dead viability assay (Fig. 6A).

Qualitative microscopic analysis showed that untreated control cells and fibroblasts exposed to all treatment conditions consistently maintained their characteristic spindle-shaped morphology, a well-established indicator of healthy, actively adherent dermal fibroblasts. In addition, we observed that the cell viability (WST-1 assay) remained high across treatment groups and even exceeded that of control cells, suggesting enhanced cellular proliferation, especially in response to HAR and Belotero Balance® (Fig. 6B).

Because qualitative imaging alone cannot fully reflect cell viability, metabolic activity of the HDFs was further quantified using the WST-1 assay (Fig. 6B). Since HAR contains niacinamide at 7.5 mg/mL, we also evaluated the cytotoxicity of free niacinamide in parallel to distinguish the effects of this ancillary active pharmaceutical ingredient (API) from those related to the hydrogel matrix itself. The resulting dose-response data demonstrated a clear inverse relationship between the

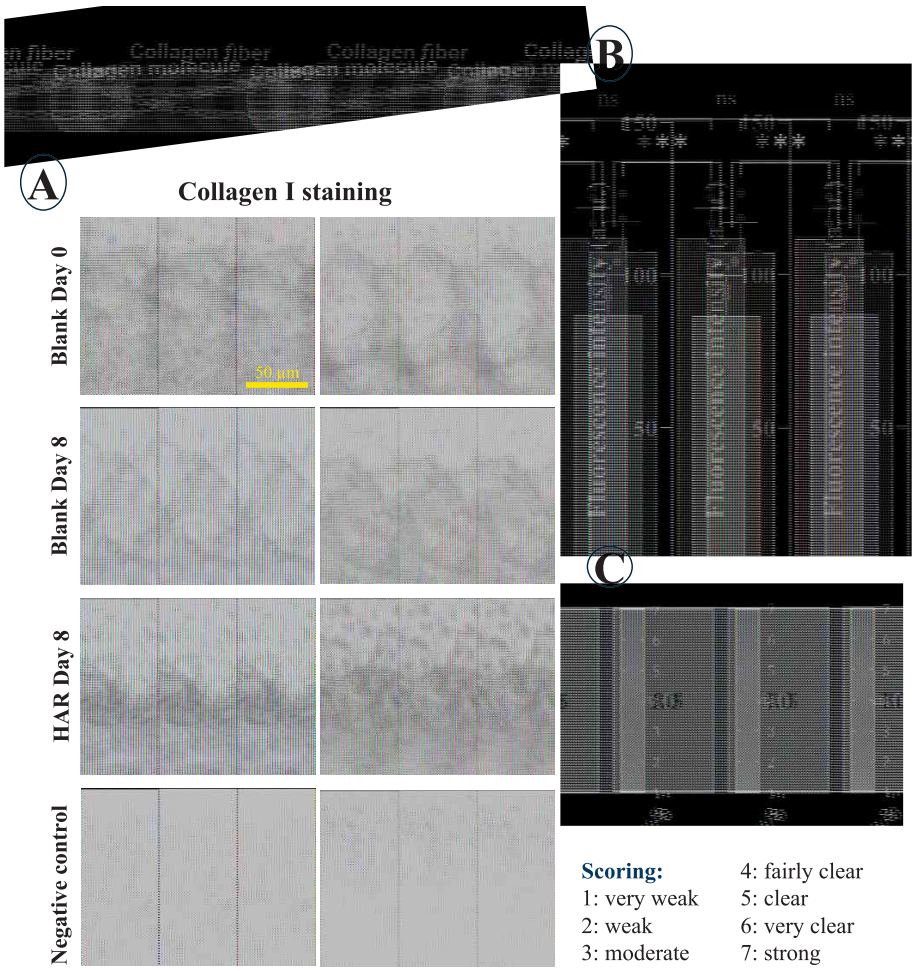

Fig. 3. *Ex vivo* collagen I content assessment. (A) Histological assessment of dermal structures of *ex vivo* skin showing the epidermis (red) and collagen I (green). Controls: untreated skin without collagen I staining at Day 0 and at Day 8; Treated: HAR treatment after 8 days. (Scale bar = 50 µm; n = 9; *ns* = not significant, ** $p \leq 0.01$, and *** $p \leq 0.001$). (B) Semi-quantitative analysis of fluorescence intensity of collagen I and (C) Expert scoring of collagen synthesis (n = 9).

free niacinamide concentration and cellular viability. Heavy cytotoxicity was observed at the highest tested concentration (15 mg/mL), resulting in a complete loss of cell viability. This concentration-dependent effect persisted down to 1.88 mg/mL, where cell viability partially recovered to approximately 80%. Full recovery of cell viability (100%) was achieved only at significantly lower concentrations of 0.94 mg/mL and 0.47 mg/mL, with this physiological viability maintained even after prolonged incubation periods of up to 5 days. In contrast, despite containing a relatively high concentration of niacinamide (7.5 mg/mL), the HAR matrix, as well as the Belotero Balance® comparator, demonstrated exceptional overall cellular biocompatibility, with quantitative viabilities exceeding 100% compared to the untreated controls.

Finally, to evaluate systemic hemocompatibility of the formulations in the unlikely event of accidental intravascular injection, an *in vitro* hemolysis assay was performed. Spectrophotometric quantification of released hemoglobin revealed minimal lytic activity against mammalian erythrocytes, with little hemolysis observed under all tested experimental conditions (Fig. 6C).

3.5. Enhanced Anti-inflammatory Effects due to HAR

To elucidate the pro-inflammatory cytokine levels of the investigated hydrogel formulations, the anti-inflammatory effects of HAR were evaluated by quantifying the levels of two key pro-inflammatory cytokines, tumor necrosis factor-alpha (TNF-α) and interleukin-6 (IL-6), in an endotoxin-stimulated murine macrophage model. As shown in Fig. 7A, exposure to free niacinamide at a concentration of 1 mg/mL resulted in a statistically significant reduction in the extracellular release of both cytokines compared with the lipopolysaccharide (LPS)-stimulated positive control.

As shown in Fig. 7A, treatment with free niacinamide effectively reduced TNF-α secretion to approximately 250 pg/mL, which is low compared with the strong inflammatory response induced by LPS stimulation (750 pg/mL). A similar anti-inflammatory effect was observed for IL-6 (Fig. 6B), where the cytokine levels in the free niacinamide group lowered to about 50 pg/mL, representing a threefold suppression relative to the LPS-stimulated control (150 pg/mL).

When the hydrogel matrices were evaluated, neither HAR nor the Belotero Balance® samples reduced TNF-α levels to the same extent as free niacinamide. Nevertheless, both fillers successfully decreased IL-6 secretion relative to the inflammatory positive control. Most notably, in direct comparison between the two dermal fillers, the niacinamide-functionalized HAR matrix proved a stronger ability to attenuate TNF-α secretion than Belotero Balance®, indicating an enhanced anti-inflammatory potential.

4. Discussion

Biostimulatory fillers aim to improve skin smoothness by restoring structural integrity at the epidermal–dermal junction and promoting ECM remodeling. Here, HAR enhanced dermal architecture, generating a denser and more organized collagen network characteristic of youthful

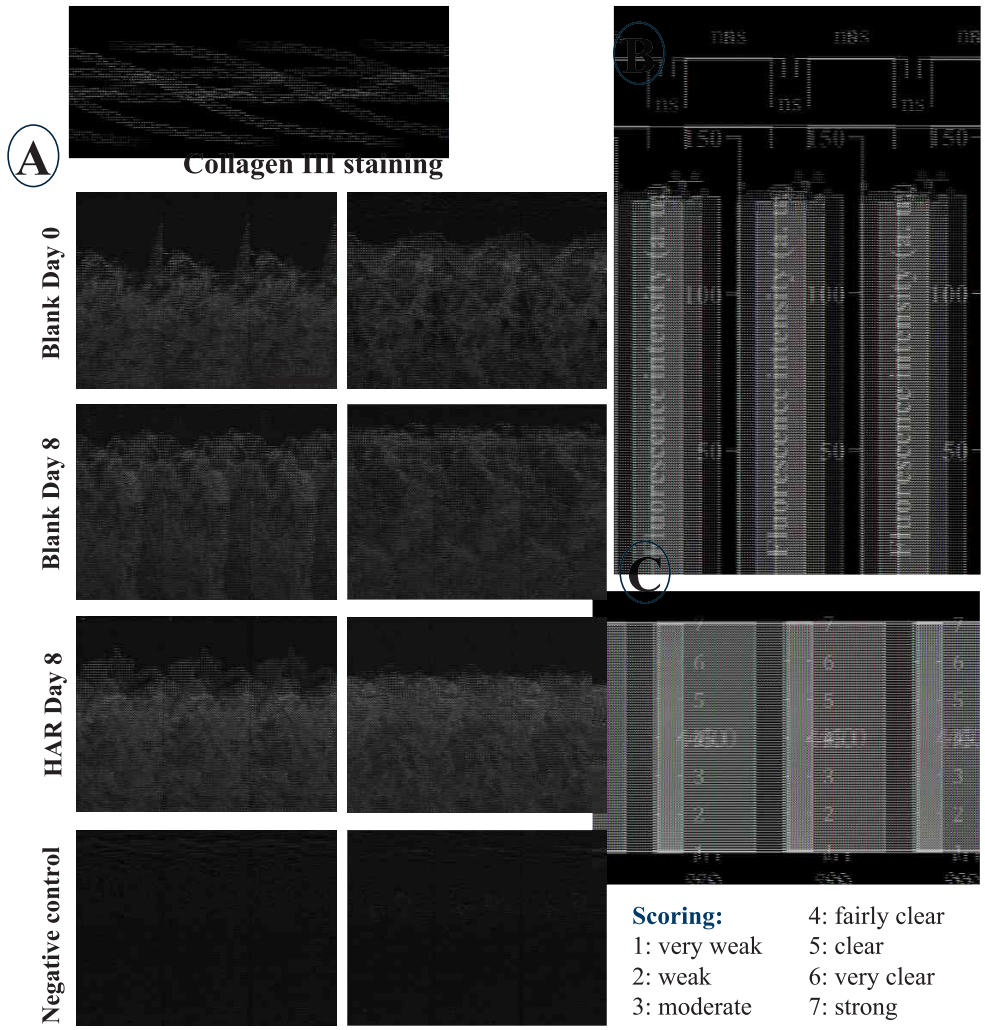

Fig. 4. *Ex vivo* collagen III content assessment. A) Histological assessment of dermal structures of *ex vivo* skin showing the epidermis with collagen III staining (pink/violet). Controls were represented by skin without collagen III staining, without treatment: blanks at Day 0 and at Day 8. Treatment with HAR after 8 days (n = 9; *ns* = not significant). Scale bar = 50 μm. B) Semi-quantitative analysis of fluorescence intensity of collagen III and C) Expert scoring of collagen synthesis (n = 9).

skin. Semi-quantitative analysis confirmed a clear increase in type I collagen. In contrast, changes in type III collagen were not significant, likely reflecting its lower abundance and slower turnover, as well as the limited 8-day *ex vivo* timeframe.

Because type III collagen naturally accounts for only about 15% of the adult dermal matrix and turns over more slowly than type I collagen, early changes in its levels are likely subtle and may fall below the detection limits of our current assay. Moreover, *ex vivo* assays primarily assess total collagen, reducing sensitivity to subtype-specific variations [36,37]. Variability in analytical approaches across studies further complicates interpretation, as some studies rely solely on qualitative visual analysis of imaging data, precluding semi-quantitative or statistical evaluation of significance [38,39]. Future investigations using standardized quantitative methods, such as ELISA or RT-qPCR, would be useful to better define collagen remodeling dynamics [40].

Skin aging is characterized by epidermal thinning and flattening of the epidermal–dermal junction [41], often accompanied by shifts in the type III/type I collagen ratio. Niacinamide, a key NAD/NADP precursor, has been shown to stimulate the synthesis of collagen types I, III, and V [19,21], supporting dermal thickening [42]. In HAR, the gradual release of niacinamide from the HA matrix is therefore expected to promote sustained, long-term collagen remodeling *in vivo*. However, the limitations of the *ex vivo* model should be considered. While short-term systems capture early biochemical changes, meaningful modulation of slower processes such as type III collagen synthesis typically requires longer observation periods. The 8-day incubation used here may therefore underestimate the full biostimulatory potential of HAR.

Beyond structural benefits, controlling the local microbiological environment is essential, as dermal injections inevitably create micro-injuries [43] that can disrupt the skin tissue and trigger inflammation. This unavoidable mechanical trauma disrupts the native skin barrier, frequently triggering mild inflammation and subsequent post-procedural complications. We therefore assessed HAR's antibacterial activity against *S. aureus* and *E. coli*. HAR exhibited selective antibacterial activity, strongly inhibiting *E. coli* proliferation while only moderately affecting *S. aureus*. This profile may provide an additional protective barrier against opportunistic bacterial contamination introduced during injection procedures. Of note, *S. aureus* asymptomatically colonizes 20–30% of the healthy adult population [44,45] and generally becomes pathogenic only under altered skin conditions [46]. Conversely, Gram-negative bacteria such as *E. coli* are not typical constituents of the skin flora [47]. These differential findings are consistent with established literature. Mathapathi *et al.* [48] tested the antibacterial effects of niacinamide against *E. coli* and *S. aureus* at 1 mg/mL, a concentration approximately seven times lower than that encapsulated within HAR. The authors reported a distinct absence of *in vitro* bactericidal activity, which they attributed to niacinamide's strict biological reliance on activating the host's innate AMPs to exert its documented

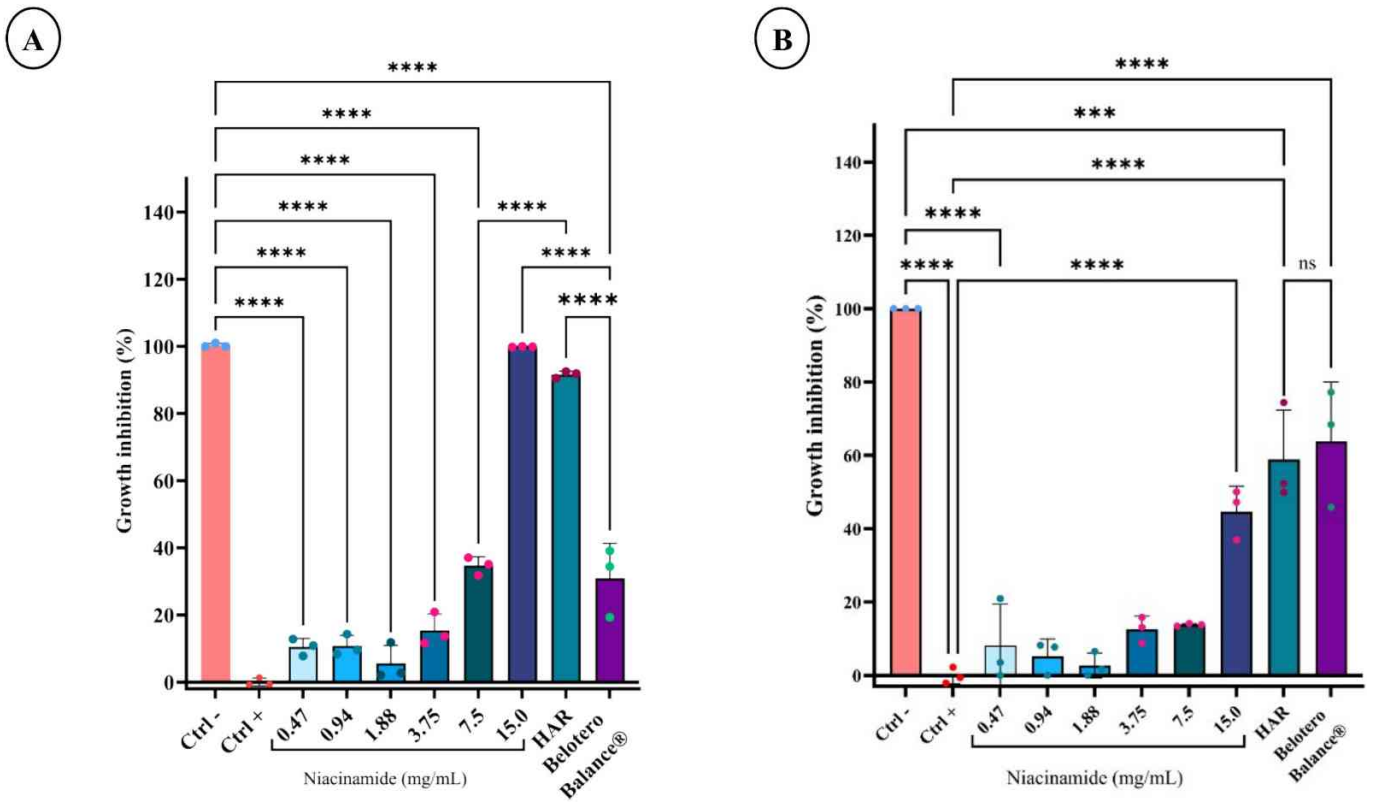

Fig. 5. Antibacterial activity assessments. Growth inhibition (%) of A) *E. coli* and B) *S. aureus* following 24 h of treatment with HAR or Belotero Balance®, compared to negative control (Ctrl-) gentamicin (1 μg/mL for *E. coli* and 4 μg/mL for *S. aureus*) and niacinamide in solution. Positive control (Ctrl+): bacteria without any treatment. Values of *** $p \leq 0.001$ and **** $p \leq 0.0001$ were considered statistically significant compared with respective controls (one-way ANOVA with Tukey's post-test (n = 3)).

antibacterial effects *in vivo* [26]. Because our highly controlled *in vitro* experimental model lacks the intact physiological immune compounds required to potentiate an AMP response, the muted efficacy against *S. aureus* remains biologically consistent. However, as a subcutaneously administered injectable, HAR will undergo gradual degradation *in vivo*, continually releasing niacinamide directly into the patient's tissues [22], likely stimulating local AMP responses and enhancing long-term defenses against *S. aureus* [48,49]. Furthermore, distinct direct mechanisms may also govern these microbial interactions. Ziklo *et al.* [25] demonstrated that niacinamide directly induces bacterial cell cycle arrest by interacting with microbial DNA at extreme concentrations (0.5 M, equivalent to 61 mg/mL). It is highly probable that at the higher concentration (*i.e.,* 15 mg/mL) utilized in our unencapsulated assay controls, this direct, DNA-binding mechanism became predominant, thereby successfully bypassing the need for an AMP-mediated pathway to achieve the profound inhibition of *E. coli* observed in our study. Notably, Ziklo *et al.* also documented a higher intrinsic physiological resistance of *S. aureus* to niacinamide compared to *E. coli*, corroborating our observed strain-specific disparities. Intriguingly, while free niacinamide at 7.5 mg/mL failed to demonstrate significant antibacterial activity against *E. coli*, the formulated HAR hydrogel, containing an equivalent niacinamide concentration, achieved growth inhibition comparable to that of gentamicin [25]. This robust functional divergence strongly indicates that the cross-linked HA matrix itself acts synergistically to mediate this effect, likely by actively preventing early bacterial adhesion and subsequently inhibiting complex biofilm formation [50].

Managing local inflammation is just as important in aesthetic treatments. Dermal microtrauma, combined with environmental stressors such as UV radiation and ROS, activate fibroblasts, keratinocytes, and tissue-resident macrophages to release pro-inflammatory cytokines, particularly TNF-α and IL-6 [17,19]. If not controlled, this ongoing inflammation can accelerate skin aging [51].

The intrinsic anti-inflammatory capacity of niacinamide is well-documented in the literature and is mechanistically linked to the suppression of the poly-(ADP-ribose) polymerase-1 (PARP-1) enzyme. The targeted inhibition of PARP-1 critically downregulates nuclear factor kappa B (NFκB) transcription, culminating in a marked, systemic decrease in pro-inflammatory cytokine levels [24]. Our *in vitro* data strictly corroborates this mechanism, explicitly demonstrating that unencapsulated niacinamide at a concentration of 1 mg/mL profoundly reduced both TNF-α and IL-6 expression relative to the robust LPS-stimulated positive control. These specific quantitative findings perfectly align with established scientific literature detailing niacinamide's specific modulatory effects on both TNF-α and IL-6 expression [7,19,52]. Interestingly, this immediate, pronounced anti-inflammatory effect was attenuated when evaluating the fully intact HAR hydrogel *in vitro*. This observation may be attributed to the encapsulation of the active niacinamide molecule within the highly crosslinked HA matrix, a structural feature that intentionally restricts the immediate bioavailability of the vitamin. Considering that the total incorporated concentration of niacinamide embedded within HAR is 7.5 mg/mL, and that a mere 1 mg/mL is sufficient to exert profound anti-inflammatory effects, it is highly reasonable to hypothesize that as the hydrogel matrix undergoes predictable, slow physiological biodegradation *in situ*, it will continuously liberate relevant concentrations of niacinamide. This controlled release mechanism could ensure a sustained, long-term anti-inflammatory effect within the dermal microenvironment.

Ensuring strong safety and biocompatibility is essential for any new dermal filler. Following direct, prolonged contact with both the HAR hydrogel and the Belotero Balance® comparator, the primary human fibroblasts consistently displayed an elongated, spindle-shaped

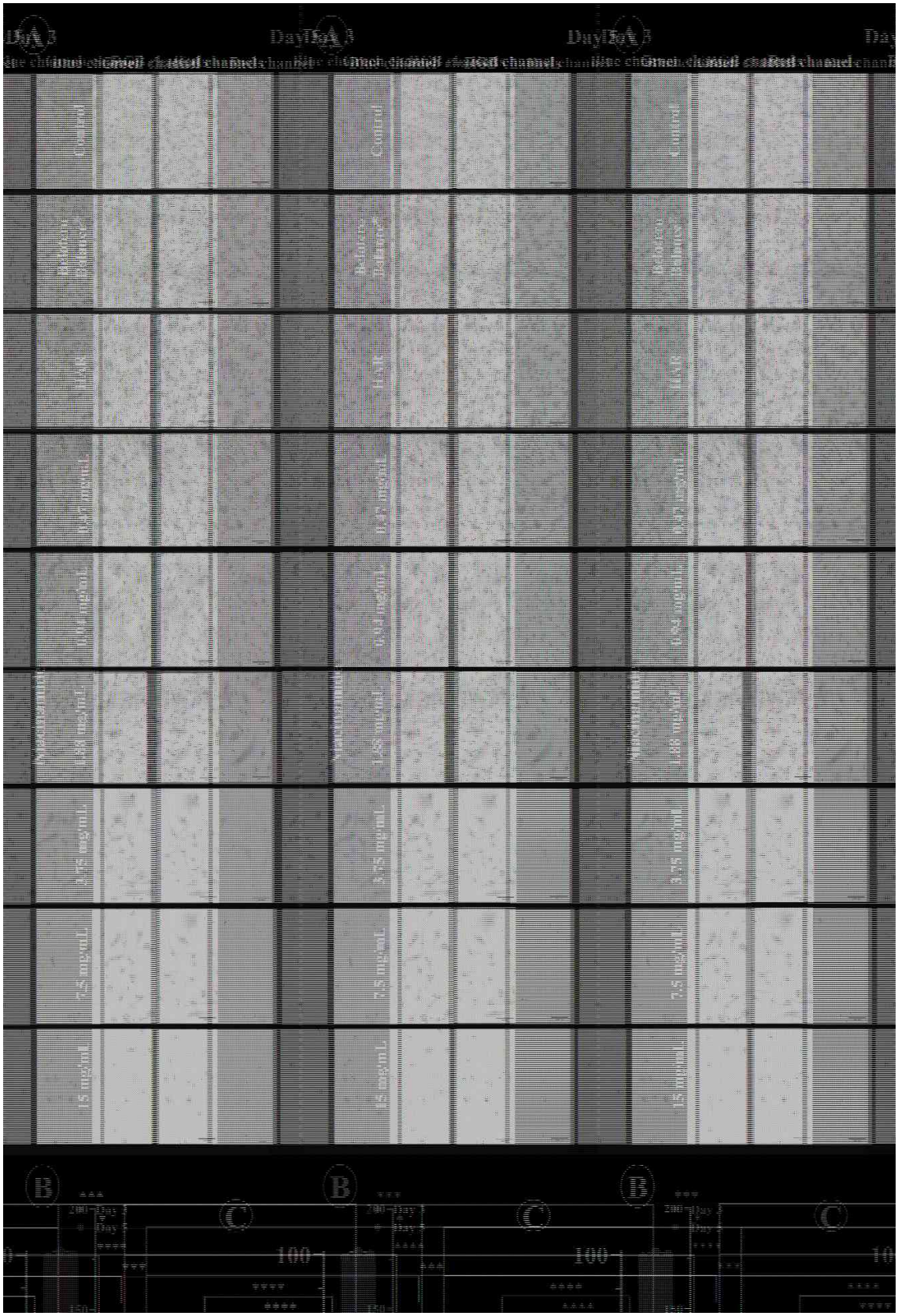

Fig. 6. Safety assessment of HAR against HDFs and RBCs. A) Safety assessment on HDFs at Days 3 and 5 using the Live/Dead assay (green channel: live cells (calcein AM); red channel: dead cells (propidium iodide); blue channel: cell nuclei (Hoescht dye), and RGB channels: overlapped (Red + Green + Blue)). Cells were treated with HAR, Belotero Balance®, and free niacinamide at 0.47, 0.94, 1.88, 3.75, 7.5, and 15.0 mg/mL. The control cells were untreated cells. Scale bar = 100 μm. B) Mitochondrial activity assessment using the WST-1 assay at Days 3 and 5 (n = 3; * $p \leq 0.05$, *** $p \leq 0.001$, and **** $p \leq 0.0001$), and C) Hemolysis assay against RBCs (n = 3).

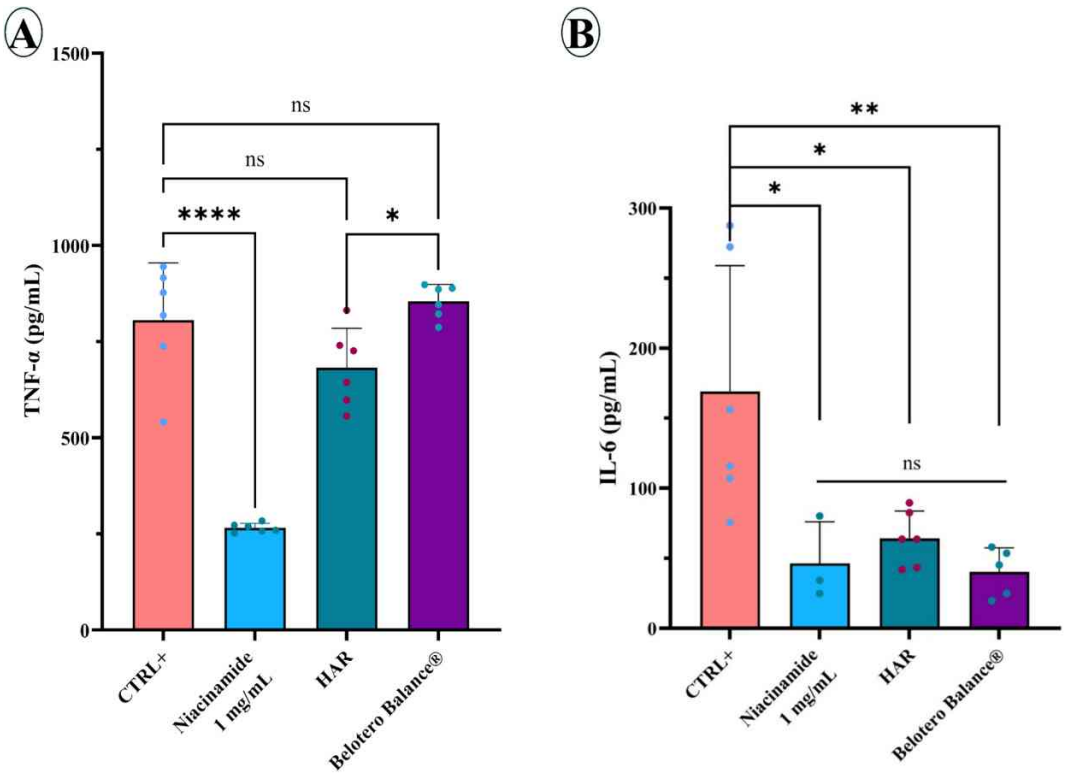

Fig. 7. Anti-inflammatory response assessments. A) TNF-α and B) IL-6 amounts (pg/mL) released by murine macrophages after treatment with either niacinamide (1 mg/mL), HAR, or Belotero Balance®. Values of * $p \leq 0.05$, ** $p \leq 0.005$, and **** $p \leq 0.0001$ were considered statistically significant compared with respective controls by one-way ANOVA followed by Bonferroni's multiple comparisons as a post-test.

morphology. This specific architectural phenotype serves as a definitive hallmark of highly viable, fundamentally healthy fibroblast cells [53].

While free niacinamide showed clear dose-dependent cytotoxicity at higher concentrations (3.75–15 mg/mL), this effect was appropriately mitigated when niacinamide was incorporated into the hydrogel. Despite containing 7.5 mg/mL of niacinamide, HAR demonstrated an excellent safety profile with no signs of cellular damage. This improved tolerance is likely due to the encapsulation of niacinamide within the crosslinked HA matrix, which limits its immediate availability to surrounding cells. By controlling the release of the active compound, the hydrogel acts as a protective delivery system, preventing acute toxicity while maintaining its biological activity.

While this study provides valuable structural and functional insights, several limitations should be considered. First, the 8-day *ex vivo* skin model restricts the ability to observe longer-term biological processes. Although changes in type I collagen organization were evident, this timeframe is likely too short to detect meaningful alterations in type III collagen, which is less abundant and remodels more slowly. *In vivo*, such changes typically require several weeks to become apparent. Additionally, the *ex vivo* design did not include a niacinamide-only or a niacinamide-free HA-vehicle arm, so the respective contributions of vitamin B3 and of the HA matrix cannot be isolated from the HAR explant data. However, in our previous *in vitro* work on the same HA-hydrogel platform, we compared the crosslinked HA comparators without vitamin B3 (*e.g.,* JUVÉDERM® VOLUMA®) and with B3 incorporation (*e.g.,* HAR-1 and HAR-3) [22]. Our previous results showed no significant difference in fibroblast collagen synthesis, indicating that vitamin B3, not the HA content, drives the bio-stimulatory readout. The explant arm was thus designed to confirm the integrated tissue-level response of the market-ready HAR product, which prior work explicitly identified as the next step.

Second, the *in vitro* antimicrobial assays do not fully replicate the complexity of human skin, particularly the role of the innate immune system and AMPs. Since niacinamide partly relies on AMP activation, especially against commensal bacteria like *S. aureus*, its true antimicrobial potential may be underestimated in this simplified model. A similar limitation applies to the anti-inflammatory findings, where the hydrogel structure restricts the immediate release of niacinamide *in vitro*.

Consequently, future studies should focus on *in vivo* and longer-term models to better capture the gradual degradation of the HA matrix and the sustained release of niacinamide. Such approaches will be essential to confirm the long-term clinical benefits of HAR, including prolonged antimicrobial protection *in vivo*, sustained anti-inflammatory effects, and enhanced collagen neogenesis required for profound skin rejuvenation.

5. Conclusion

Niacinamide has firmly established itself as a highly versatile, multifunctional molecule within the contemporary anti-aging cosmetic arsenal. Beyond its immediate biochemical utility, it offers profound long-term potential, including robust antioxidant defense, the mitigation of cellular stress, comprehensive anti-aging properties, and significant wrinkle reduction. The present comparative investigation rigorously demonstrates that encapsulating this potent molecule within a highly crosslinked HA matrix—formulated as the novel dermal filler, HAR—yields a highly synergistic functional profile.

Our *in vitro* and *ex vivo* analyses conclusively show that HAR actively drives profound dermal biostimulation by densifying and reorganizing the fibrillar collagen network. Furthermore, the functionalized hydrogel provides crucial prophylactic value, exhibiting selective, highly potent antibacterial activity against potential bacterial contaminants such as *E. coli*. Crucially, the crosslinked nature of the HAR hydrogel actively buffers the dose-dependent cytotoxicity inherent to high concentrations of free niacinamide, preserving exceptional cellular biocompatibility

while establishing a mechanism for controlled, sustained molecular release. This gradual biodegradation is hypothesized to ensure the long-term, continuous downregulation of pro-inflammatory mediators, notably TNF-α and IL-6, within the dermal microenvironment following the inevitable micro-trauma of injection.

Consequently, HAR emerges as a functionally superior, highly biocompatible dermal filler that bares the potential to successfully elevate traditional aesthetic approaches. Overall, it functions as a sophisticated, dual-action medical device capable of delivering immediate mechanical tissue support and physical volumization, seamlessly paired with the long-term, progressive regenerative benefits governed by the sustained local bioavailability of niacinamide.

CRediT authorship contribution statement

Alexandre Porcello: Writing – review & editing, Writing – original draft, Visualization, Validation, Project administration, Methodology, Investigation, Data curation, Conceptualization. **Cindy Schelker:** Writing – review & editing, Investigation, Data curation, Conceptualization. **Olivier Jordan:** Writing – review & editing, Visualization, Validation, Methodology, Investigation, Funding acquisition, Formal analysis. **Karl Perron:** Writing – review & editing, Visualization, Investigation, Formal analysis. **Emmanuelle Sublet:** Writing – review & editing, Investigation, Formal analysis. **Cíntia Cristina Santi Martignago:** Writing – review & editing, Visualization, Investigation, Formal analysis. **Cintia Marques:** Writing – review & editing, Investigation. **Lee Ann Applegate:** Writing – review & editing, Resources, Investigation. **Alexis Emmanuel Laurent:** Writing – review & editing, Resources, Conceptualization. **Viorica Patrulea:** Writing – review & editing, Visualization, Validation, Supervision, Resources, Methodology, Investigation, Funding acquisition, Formal analysis, Data curation, Conceptualization.

Declaration of competing interest

The authors declare the following financial interests/personal relationships which may be considered as potential competing interests: AP, CS and CM are part-time employees of Louna Regenerative, the manufacturer and patent holder of the HAR dermal filler evaluated in this study. Despite this commercial affiliation, the funders had no direct role in the independent collection, analysis, or interpretation of the experimental data, nor did they exert editorial control over the writing of the manuscript or the final decision to publish these results.

Acknowledgments

The authors gratefully acknowledge the material support provided by Louna Regenerative, which supplied the HAR hydrogel, alongside the standardized syringes and needles utilized in the *ex vivo* dermal injection protocols. We would like to thank the Laboratoire EUROFINS BIO-EC for their expert technical assistance and support throughout the histological processing and immunofluorescence imaging phases of this investigation. The authors thank Dr. Geoffrey Depaepe (University of Geneva) for his kind assistance during the hemolysis assay. Mr Tayeb Jbilou (University of Geneva) is acknowledged for his kind assistance during CPD and SEM analysis. Office de Promotion des Industries et des Technologies (OPI), Geneva, Switzerland, is acknowledged for their financial support (Project: “Dynamiser la régénération de la peau”).

Data availability

Data will be made available upon request.

References

[1] R.M. Ortiz-Flores, et al., Enhanced Facial Rejuvenation: Biostimulatory Effects of Hylan Gel Dermal Filler DX on Collagen Synthesis and Tissue Regeneration, Aesthetic Plast Surg 50 (2) (2026) 707–725.
[2] K. Pfisterer, L.E. Shaw, D. Symmank, W. Weninger, The Extracellular Matrix in Skin Inflammation and Infection, Front Cell Dev Biol 9 (2021) 682414.
[3] D. Cassuto, G. Bellia, C. Schiraldi, An Overview of Soft Tissue Fillers for Cosmetic Dermatology: From Filling to Regenerative Medicine, Clin Cosmet Investig Dermatol 14 (2021) 1857–1866.
[4] S. Huang, et al., Quantitative Nanohistology of Aging Dermal Collagen, Front. Aging 4 (2023) 1178566.
[5] V. Bhardwaj, et al., Holistic Approach to Visualize and Quantify Collagen Organization at Macro, Micro, and Nano-Scale, Skin Res Technol 28 (3) (2022) 419–426.
[6] D.M. Reilly, J. Lozano, Skin Collagen through the Lifestages: Importance for Skin Health and Beauty, Plast Aesthet Res 8 (2021) 2.
[7] H. Lee, Y. Hong, M. Kim, Structural and Functional Changes and Possible Molecular Mechanisms in Aged Skin, Int J Mol Sci 22 (22) (2021) 12489.
[8] A.C. Franco, C. Aveleira, C. Cavadas, Skin senescence: mechanisms and impact on whole-body aging, Trends Mol Med 28 (2) (2022) 97–109.
[9] J.W. Shin, S.H. Kwon, J.Y. Choi, J.I. Na, C.H. Huh, H.R. Choi, K.C. Park, Molecular Mechanisms of Dermal Aging and Antiaging Approaches, Int J Mol Sci 20 (2019) 2126.
[10] Z. Qin, R.M. Balimunkwe, T. Quan, Age-related reduction of dermal fibroblast size upregulates multiple matrix metalloproteinases as observed in aged human skin in vivo, Br J Dermatol 177 (2017) 1337–1348.
[11] T. Ahmed, et al., Combining Nano-Physical and Computational Investigations to Understand the Nature of Aging in Dermal Collagen, Int J Nanomedicine 12 (2017) 3303–3314.
[12] D.A. Lintzeri, N. Karimian, U. Blume-Peytavi, J. Kottner, Epidermal thickness in healthy humans: A systematic review and meta-analysis, J Eur Acad Dermatol Venereol 36 (2022) 1191–1200.
[13] B. Lynch, et al., A Mechanistic View on the Aging Human Skin through Ex Vivo Layer-by-Layer Analysis of Mechanics and Microstructure of Facial and Mammary Dermis, Sci Rep 12 (1) (2022) 849.
[14] R.D. Wagner, A. Fakhro, J.A. Cox, S.A. Izaddoost, Etiology, prevention, and management of infectious complications of dermal fillers, Semin Plast Surg 30 (2016) 83–86.
[15] A.E. Gehrke, C. Giai, M.I. Gomez, Staphylococcus aureus Adaptation to the Skin in Health and Persistent or Recurrent Infections, Antibiotics 12 (10) (2023) 1520.
[16] L. Christensen, V. Breiting, M. Janssen, J. Vuust, E. Høgdall, Adverse reactions to injectable soft tissue permanent fillers, Aesthetic Plast Surg 29 (2005) 34–48.
[17] N. Philips, H. Siomyk, D. Bynum, S. Gonzalez, Skin Cancer, Polyphenols, and Oxidative Stress, in: V. Preedy (Ed.), Cancer, Academic Press, San Diego, 2014, pp. 265–270.
[18] D.A. Yanez, R.K. Lacher, A. Vidyarthi, O.R. Colegio, The role of macrophages in skin homeostasis, Pflügers Arch 469 (2017) 455–463.
[19] N. Philips, J. Chalensouk-Khaosaat, S. Gonzalez, Stimulation of Fibrillar Collagen and Heat Shock Proteins by Nicotinamide or Its Derivatives in Non-Irradiated or UVA-Radiated Fibroblasts and Direct Antioxidant Activity of Nicotinamide Derivatives, Cosmetics 2 (2) (2015) 146–161.
[20] G.R. Guimarães, P.P. Almeida, S.L. de Oliveira, L.P. Rodrigues, J.L. de Carvalho, M. Boroni, Hallmarks of aging in macrophages: Consequences to skin inflammaging, Cells 10 (2021) 1323.
[21] Q. Wessels, et al., The Potential of a Niacinamide-Dominated Cosmeceutical Formulation on Fibroblast Activity and Wound Healing In Vitro, Int Wound J. 11 (2) (2014) 152–158.
[22] A. Porcello, et al., Dual Functionalization of Hyaluronan Dermal Fillers with Vitamin B3: Efficient Combination of Bio-Stimulation Properties with Hydrogel System Resilience Enhancement, Gels 10 (6) (2024) 361.
[23] C. Marques, F. Hadjab, A. Porcello, K. Lourenço, C. Scaletta, P. Abdel-Sayed, N. Hirt-Burri, L.A. Applegate, A. Laurent, Mechanistic insights into the multiple functions of niacinamide: Therapeutic implications and cosmeceutical applications in functional skincare products, Antioxidants 13 (2024) 425.
[24] M. Joshi, et al., Modulatory Role of Vitamins A, B3, C, D, and E on Skin Health, Immunity, Microbiome, and Diseases, Pharmacol Rep. 75 (5) (2023) 1096–1114.
[25] N. Ziklo, et al., Niacinamide Antimicrobial Efficacy and Its Mode of Action via Microbial Cell Cycle Arrest, Microorganisms 12 (8) (2024) 1581.
[26] J. Hakansson, et al., Characterization of the In Vitro, Ex Vivo, and In Vivo Efficacy of the Antimicrobial Peptide DPK-060 Used for Topical Treatment, Front Cell Infect Microbiol 9 (2019) 174.
[27] G. Brianezi, F. Grandi, E. Bagatin, M.M. Enokihara, H.A. Miot, Dermal type I collagen assessment by digital image analysis, An Bras Dermatol 90 (2015) 723–727.
[28] O. Jordan, B.H. Gan, S. Alwan, K. Perron, E. Sublet, V. Ducret, H. Ye, G. Borchard, J.-L. Reymond, V. Patrulea, Highly potent cationic chitosan derivatives coupled to antimicrobial peptide dendrimers to combat Pseudomonas aeruginosa, Adv Healthc Mater 13 (2024) e2304118.
[29] J. Campbell, High-throughput assessment of bacterial growth inhibition by optical density measurements, Curr Protoc Chem Biol 3 (2011) 100–115.
[30] P. Micheels, A. Porcello, T. Bezzola, D. Perrenoud, P. Quinodoz, Y. Kalia, E. Allémann, A. Laurent, O. Jordan, Clinical Perspectives on the Injectability of Cross-Linked Hyaluronic Acid Dermal Fillers: A Standardized Methodology for Commercial Product Benchmarking with Inter-Injector Assessments, Gels 10 (2) (2024) 101.

[31] C. De la Guardia, A. Virno, M. Musumeci, A. Bernardin, M.B. Silberberg, Rheologic and physicochemical characteristics of hyaluronic acid fillers: Overview and relationship to product performance, Facial Plast Surg 38 (2022) 116–123.
[32] W. Zhu, M. da Silva, G. Murray, C.A. Dreiss, Integrated mechanical and structural characterisation of 24 commercial hyaluronic acid fillers: A multi-parametric framework for comparative analysis, J. Colloid Interface Sci 713 (2026) 140085.
[33] Raquel Fernández de Castro Isalguez, Safe Facial Rejuvenation with PEGylated Fillers in a Complex Oncology Case, JOJ Dermatol & Cosmet 7 (1) (2025) 555704.
[34] T. Hino, J.L. Ford, Effect of nicotinamide on the properties of aqueous HPMC solutions, Int J Pharm 226 (2001) 53–60.
[35] E. Dănilă, et al., Formulation and Characterization of Niacinamide and Collagen Emulsion and Its Investigation as a Potential Cosmeceutical Product, Cosmetics 11 (2) (2024) 40.
[36] J. Asserin, E. Lati, T. Shioya, J. Prawitt, The effect of oral collagen peptide ation on skin moisture and the dermal collagen network: Evidence from an ex vivo model and randomized, placebo-controlled clinical trials, J Cosmet Dermatol 14 (2015) 291–301.
[37] M. Narda, C. Trullas, A. Brown, et al., Glycolic acid adjusted to pH 4 stimulates collagen production and epidermal renewal without affecting levels of proinflammatory TNF-alpha in human skin explants, J Cosmet Dermato. 20 (2021) 513–521.
[38] L. Nakab, C.K. Hee, O. Guetta, Improvements in skin quality biological markers in skin explants using hyaluronic acid filler VYC-12L, Plast Reconstr Surg Glob Open 8 (2020) e2723.
[39] W. Xu, S.J. Hong, S. Jia, Y. Zhao, R.D. Galiano, T.A. Mustoe, Application of a partial-thickness human ex vivo skin culture model in cutaneous wound healing study, Lab Investig 92 (2012) 584–599.
[40] S. Gou, Y.N. Kalia, Development of an ex vivo human skin model and evaluation of biological responses to subcutaneously injected hyaluronic acid formulations, Int J Pharm 674 (2025) 125490.
[41] J. Khavkin, D.A. Ellis, Aging Skin: Histology, Physiology, and Pathology, Facial Plast Surg Clin North Am 19 (2) (2011) 229–234.
[42] W. Gehring, Nicotinic Acid and Niacinamide and the Skin, J. Cosmet Dermatol 3 (2) (2004) 88–93.
[43] E. Haneke, Managing Complications of Fillers: Rare and Not-So-Rare, J Cutan Aesthet Surg 8 (4) (2015) 198–210.
[44] S. Sommatis, et al., Biological Efficacy Evaluation of a Non-Cross-Linked Hyaluronic Acid Dermal Filler for Biomedical Application in Inflammatory Scalp Conditions, Life 12 (1) (2021) 2.
[45] J.U. Sollid, et al., Staphylococcus aureus: Determinants of Human Carriage, Infect Genet Evol 21 (2014) 531–541.
[46] P. Duckney, et al., The Role of the Skin Barrier in Modulating the Effects of Common Skin Microbial Species on the Inflammation, Differentiation and Proliferation Status of Epidermal Keratinocytes, BMC Res Notes 6 (1) (2013) 474.
[47] K. Chiller, B.A. Selkin, G.J. Murakawa, Skin Microflora and Bacterial Infections of the Skin, J Investig Dermatol Symp Proc 6 (3) (2001) 170–174.
[48] M.S. Mathapathi, et al., Niacinamide Leave-On Formulation Provides Long-Lasting Protection against Bacteria In Vivo, Exp Dermatol 26 (9) (2017) 827–829.
[49] V. Losasso, K. Agarwal, M. Waskar, A. Majumdar, J. Crain, M. Winn, M. Hoptroff, Small molecules enhance the potency of natural antimicrobial peptides, Biophys J 121 (2022) 491–501.
[50] C. Romanò, et al., Hyaluronic Acid and Its Composites as a Local Antimicrobial or Antiadhesive Barrier, J Bone Joint Infect 2 (1) (2017) 63–72.
[51] J.E. Oblong, et al., Metabolic Dysfunction in Human Skin: Restoration of Mitochondrial Integrity and Metabolic Output by Nicotinamide in Primary Dermal Fibroblasts from Older Donors, Aging Cell 19 (10) (2020) e13248.
[52] Y.C. Boo, Mechanistic Basis and Clinical Evidence for the Applications of Nicotinamide to Control Skin Aging and Pigmentation, Antioxidants 10 (8) (2021) 1315.
[53] W.I. Choi, et al., An Injectable and Physical Levan-Based Hydrogel as a Dermal Filler for Soft Tissue Augmentation, Biomater Sci 6 (10) (2018) 2627–2638.